공학석사학위논문

산업용 로봇 고장 진단을 위한 암묵신호 분리 기반 다축 간섭 최소화 기법

Minimization of Multi-Axis Interference for Fault Detection of Industrial Robots Based on Blind Source Separation

2019년 8월

서울대학교 대학원

기계항공공학부

YUAN HAO

산업용 로봇 고장 진단을 위한 암묵신호 분리 기반 다축 간섭 최소화 기법

Minimization of Multi-Axis Interference for Fault Detection of Industrial Robots Based on Blind Source Separation

지도교수 윤 병 동

이 논문을 공학석사 학위논문으로 제출함

2019년 4월

서울대학교 대학원

기계항공공학부

YUAN HAO

YUAN HAO의 공학석사 학위논문을 인준함

2019년 6월

위 원 장 ______조 맹 효______ (인)

부위원장 ______윤 병 동______ (인)

위 원 ______김 도 년______ (인)

Abstract

Minimization of Multi-Axis Interference for Fault Detection of Industrial Robots Based on Blind Source Separation

YUAN HAO

School of Mechanical and Aerospace Engineering

The Graduate School

Seoul National University

As smart factory is becoming popular, industrial robots are highly demanding in many manufacturing fields for factory automation. Unpredictable faults in the industrial robot could bring about interruptions in the whole manufacturing process. Therefore, many methods have been developed for fault detection of the industrial robots. Because gearboxes are the main parts in the power transmission system of industrial robots, fault detection of the gearboxes has been widely investigated. Especially, vibration analysis is a well-established technique for fault detection of the industrial robot gearbox.

However, the vibration signals from the gearboxes are mixed convolutively and linearly at each axes, which makes it difficult to locate a damaged gearbox, and reduce fault detection performance. Thus, this paper develops a vibration signal separation technique for fault detection of industrial robot gearboxes under multi-axis interference. The developed method includes two steps, frequency domain independent component analysis (ICA-FD) and time domain independent component analysis (ICA-TD). ICA-FD is aimed at separating convolutive mixture of signals, and ICA-TD is aimed at eliminating the residual mixed components.

The experiment is performed to demonstrate the effectiveness of the proposed method. The results show that the proposed method could successfully separate the mixed signals by obtaining vibration signals from each gearbox, and enhance fault detection performance for the industrial robot gearboxes.

Keyword: Fault detection

Industrial robot

Multi-Axis Interference

Signal separation

Independent component analysis

Student Number: 2017-22579

Table of Contents

List of Figures

Nomenclature

A	Mixing matrix in ICA-TD
a_{ij}	Coefficient from $s_j(t)$ to $x_i(t)$
BSS	Blind source separation
$b_{ji}(\tau)$	Impulse response in separation process
c-FastICA	Fast fixed-point algorithm for independent component analysis of complex valued signals
FastICA	Fast fixed-point algorithm for independent component analysis
G	Non-quadratic function
$h(\tau)$	Mixing matrix in ICA-FD
$H(y)$	Differential entropy with the definition
ICA	Independent component analysis
ICA-FD	Frequency domain independent component analysis
ICA-TD	Time domain independent component analysis
MSICA	Multi-stage independent component analysis
$h_{ij}(\tau)$	Impulse response from source j to sensor i
$h_{ij}(f)$	Impulse response in frequency domain
$J(y)$	Non-Gaussianity feature
$powRatio_i(n,f)$	Power ratio between i-th separated signal and power sum of all separated signals
s	Vector of independent source signals
$s_j(t)$	Independent source signals
$s_j(n,f)$	STFT result of $s_j(t)$
$S(k,f)$	Independent source signals in frequency domain
W	Separation matrix
x	Vector of measured signals
$x_i(t)$	Measured signals
$x_i(n,f)$	STFT result of $x_i(t)$

$X(k,f)$	Measured signals in frequency domain
y	Estimation of independent source signals
y_{Gauss}	A Gaussian random variable which has same covariance matrix with y
$Y(k,f)$	Estimated signals in frequency domain
ρ	Correlation coefficient between two real-valued sequences
$\Gamma\left(\{c_k\},\{\Pi_f\}\right)$	Cost function in global optimization in permutation process

Chapter 1. Introduction

1.1 Background and Motivation

With the development of Industrial 4.0, smart factory becomes popular all over the world. And industrial robots play a significant role in the automation of manufacturing processes in smart factory [1]. The industrial robots have larger bearing capacity than human workers, and can operate in complex environment [2]. The global industrial robotics market is expected to achieve $70.7 billion in 2023, and it grew from $37.9 billion with a compound annual growth rate (CAGR) of 9.4% from 2017 to 2023 [3]. However, nowadays, there are huge amount of downtime loss in manufacturing processes due to unexpected faults of industrial robots. One survey estimated downtime cost in the automotive industry at an average of $22,000 per minute [4, 5]. Therefore, many fault detection techniques have been developed for industrial robots to solve the problem [6].

1.2 Scope of Research

Failures in industrial robots are resulting from both electronic [7] and mechanical components [8]. Approximately 45% of failures are from mechanical problems [9]. And gearbox is an important composition of the mechanical components in industrial robots. Fault detection of gearboxes have also been investigated [10-12]. Especially, vibration analysis is a well-established technique for fault detection of the industrial robot gearbox. Erik Olsson et al. [13] used acoustic signals and case-based reasoning to diagnose the faults in industrial robot, which initiated the vibration analysis in industrial robot. Ikbal Eski et al. [14] applied artificial neural networks to detect faults on robot manipulators.

However, the vibration signals from each gearbox can be mixed each other in the diagnostic methods because industrial robots usually have multiple axes. The mixed signals make it difficult to locate a damaged gearbox, and reduces fault detection performance. Thus, it is important to separate the mixed signals for fault detection of gearboxes in industrial robots. Gelle et al. [15] developed blind source separation (BSS) into acoustical and vibration analysis of rotating machines. The experiments were based on simple mechanism. Xinhao Tian et al. [16] utilized independent component analysis (ICA) in the frequency domain and wavelet filtering to do gearbox fault diagnosis, which took ICA into complex mechanism fault detection. Leng et al. [17] combined ensemble empirical mode decomposition (EEMD) and constrained independent component analysis (CICA), which can extract fault features based on single-channel signal. However, those studies were only limited to vibration separation of different components in a single gearbox, and have not been applied to multiple gearboxes in industrial robots.

Independent component analysis (ICA) is one of the blind source separation techniques that has been used for feature extraction and signal separation in speech recognition [18], medical signal processing [19] and machinery condition monitoring [20]. Lisa J. Stifelman [21] first introduced the cocktail party effect in auditory interfaces, which took blind source separation into research field. Then, a fast fixed-point algorithm for independent component analysis (FastICA) was introduced by Aapo Hyvärinen and Erkki Oja [22, 23]. FastICA can separate linearly mixed time series with low accuracy. E. Bingham and A. Hyvärinen [24] proposed a fast fixed-point algorithm for independent component analysis of complex valued signals (c-FastICA). To separate the signals in reverberant condition, Tsu Nishikawa et al. [25] proposed multistage ICA (MSICA) method for blind source separation. It used frequency domain ICA method (ICA-FD) to solve convolutive BSS problems. In addition, time domain ICA method (ICA-TD) was used to solve residual crosstalk components problem. The basic structure of MSICA method are demonstrate in Figure 1-2.

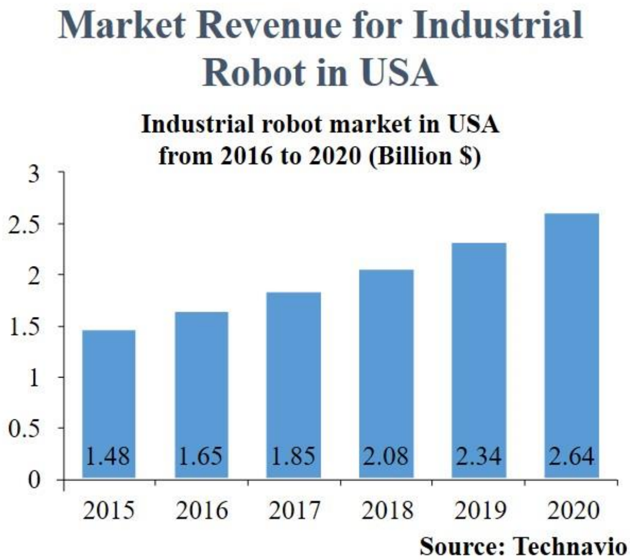

Figure 1-1 Market Revenue for Industrial Robot in USA

In this paper, we develop MSICA method into fault detection of gearboxes in industrial robots. In industrial robots, because the distances between gearboxes are different, and the size of gearboxes are various. If the distance between two gearboxes is small and the two gearboxes are large which makes the distance is resembling to the size of gearboxes, the vibration signals from gearboxes will be convolutively and linearly mixed. Because the largest and shortest distance between gearbox components are quite different. And convolutive signal mixing problems arise when there is time delay between signals from large distance signal propagation or reflections [26]. Linear mixing problems arise when the time delay approach to zero. Therefore, some vibration signal in the industrial robot are convolutively mixed, and some are linearly mixed.

Thus, multistage ICA method is efficient to separate the mixed signals in the industrial robots. The first stage is ICA-FD, which can separate convolutive mixed vibration signals and the second stage is ICA-TD, which can separate linearly mixed signals, and also deal with residual mixed components. After the separation of vibration signals, root mean square (RMS) is calculated by extracting constant speed parts of the measured vibration signals to quantify the fault severity. The diagnosis results are obtained from from RMS feature calculation.

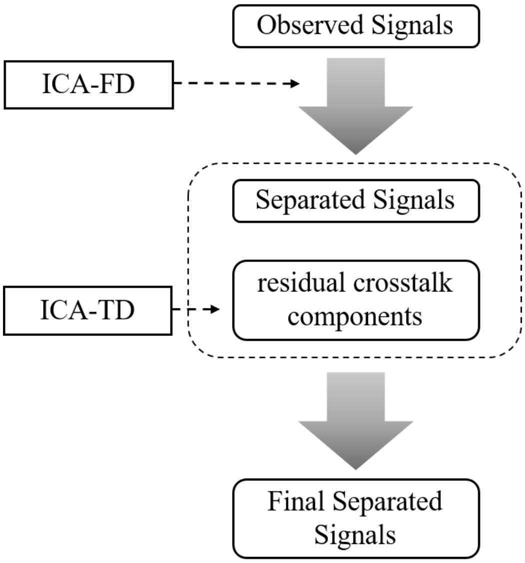

Figure 1-2 Structure of Multi-Stage Independent Component Analysis (MSICA)

1.3 Structure of the Thesis

The rest of the paper is structured as follows. The structure of industrial robot is introduced in Chapter 2. The analytical theories of ICA-TD, ICA-FD and MSICA are introduced firstly in Chapter 3. In Chapter 4, the performance of the developed technique is then experimentally evaluated on the base of using industrial robot vibration data signals measured from gearboxes of an industrial robot. And conclusions and future work are summarized in Chapter 5.

Chapter 2. Structure of Industrial Robot

2.1 Structure of Experimental Robot

Figure 2-1(a) shows a six-axis industrial robot and Figure 2-1(b) shows its 4th axis and 5th axis. Six gearboxes and motors are located in each axis to drive the movements. Every axis can rotate by 360°. Vibration arises from gear mesh and bearing rotation in gearboxes when axes have movements. Because the weights and scales are different in arms, the amplitudes of vibration in each gearbox are different.

To detect vibration signals from gearboxes, six vibration sensors are attached on each gearbox. The sensors can observe vibration signals by relative displacements between the inertia mass and the shell in sensors. As shown in Figure 2-1(b), two vibration sensors are attached on 4th gearbox and 5th gearbox. The vibration signals detected from sensors are used to calculate features for fault diagnosis. The distance between two gearboxes is small and the sizes of gearboxes are large. Therefore, the vibration can influence each other in these axes.

Thus, the vibration signals detected from sensors are mixed signals. In robot fault detection process, measured signals are need to calculate diagnosis features. The detected vibration signals cannot be used if they are mixed signals. Therefore, the mixed vibration signals should be separated into source signals. After separation, the correct information can be obtained from the source signals.

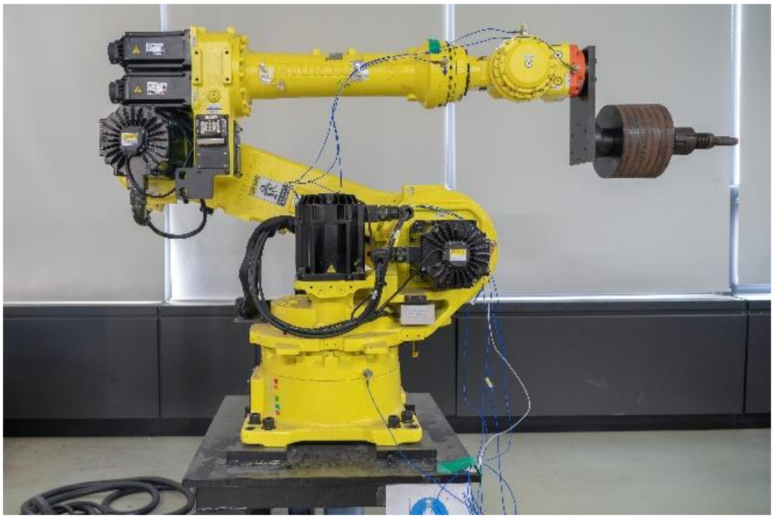

(a)

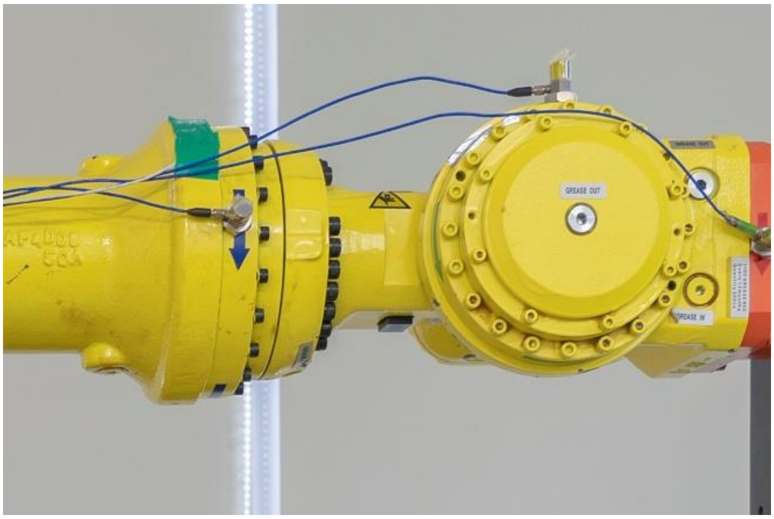

(b)

Figure 2-1 (a) Experiment industrial robot, and (b) its 4th axis and 5th axis

2.2 Problem in Industrial Robot Fault Detection

As shown in Figure 2-2, in the industrial robot, especially 4th axis and 5th axis. Two vibration sensors are attached on both gearboxes separately. When using sensors to obtain signals, the signals from the 4th and 5th gearbox will be mixed into sensors. Also, the root mean square (RMS) is calculated from detected vibration signals. As shown in Figure 2-2, the faulty component exists in 4th gearbox. However, if RMS is calculated in 4th gearbox single motion mode when there is only 4th axis rotating, RMS result shows that 4th gearbox is faulty. And RMS result in 5th gearbox single motion mode shows that 5th gearbox is in normal condition. But when calculating RMS feature in multi-axis motion, RMS result shows that both 4th gearbox and 5th gearbox are faulty. Thus, this signal mixing problem can influence the fault detection results. This vibration signal mixing problem in industrial robot fault detection can be defined as multi-axis interference. Therefore, to separate the sensor signals, blind source separation method can be applied into vibration signals mixing problem.

The multi-axis interference is disparate in different industrial robots, because the lengths of arms are variable and also the weight varies. Furthermore, in experimental industrial robot, due to the longer length between 4th and 5th axes, the vibration signals are convolutively and linearly mixed. Therefore, the mixed signals should be separated in frequency domain firstly. And because the distances of the components of 4th gearbox and 5th gearbox are different, there can be residual mixed components after separation in frequency domain. Then time domain separation can be applied in order to deal with the residual mixed components.

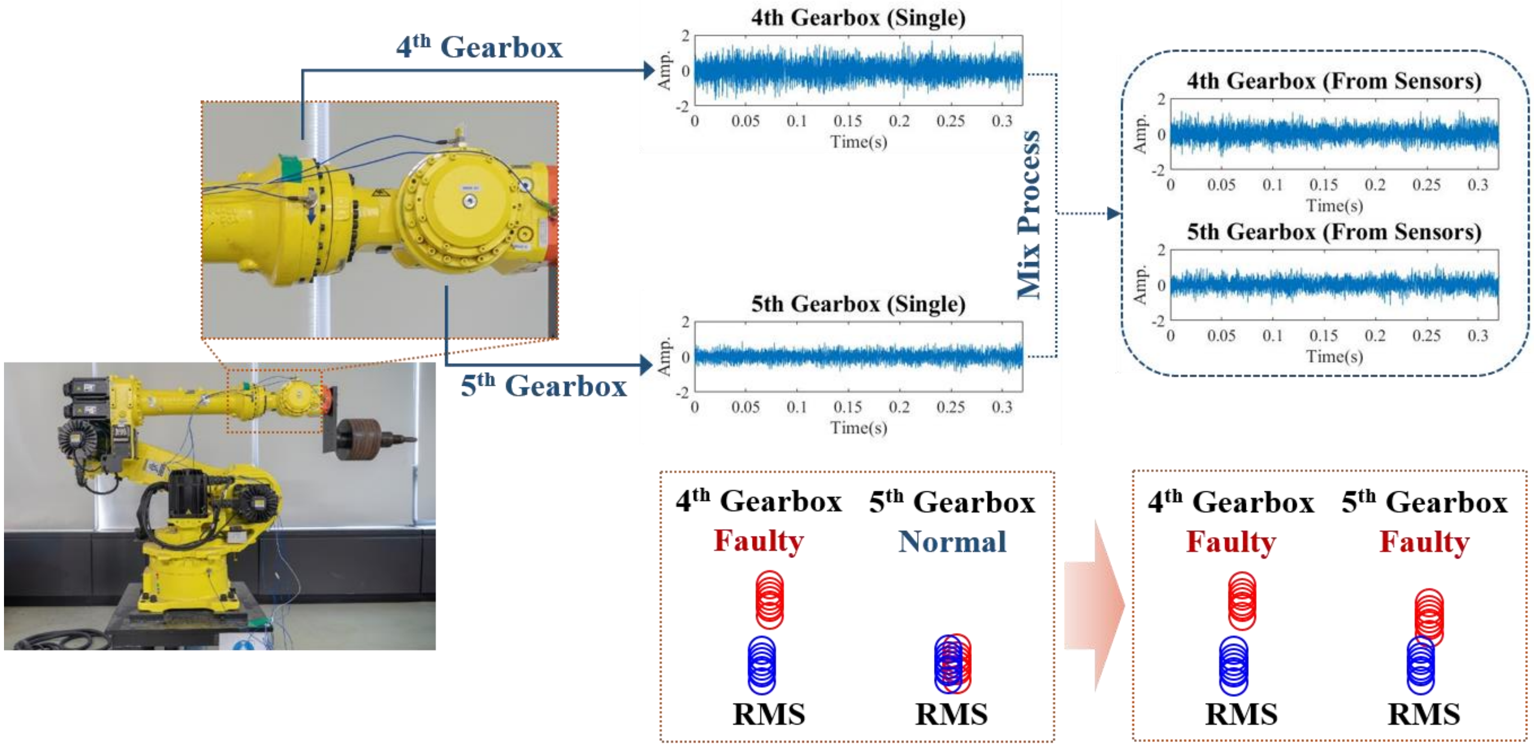

Figure 2-2 Signal mixing problem in industrial robots

Chapter 3. Methodology

3.1. Time Domain Independent Component Analysis (ICA-TD)

Time domain independent component analysis (ICA-TD) is a method that can find underlying signals from a set of mixed signals in time domain. ICA-TD is suitable to separate linear signal mixtures. It considers measured multi-channel signals as a mixture of independent component signals. In ICA-TD, preprocessing is needed which includes centering and whitening. Centering process is responsible for transferring the vibration data into the zero mean valued signals. And whitening process is to making the signals have unity variances. After preprocess, separation process is introduced below.

If we define $s_j(t)$ the independent component signals and define $x_i(t)$ the measured mixed signals. The measured signals can be expressed as below

$$x_i(t) = \sum_{j=1}^{N} a_{ij} * s_j(t) \tag{3.1}$$

where j is the serial number of the independent component signals ($1 \leq j \leq N$), i is the serial number of the measured multi-channel signals ($1 \leq i \leq M$) and a_{ij} is the unknown coefficient from $s_j(t)$ to $x_i(t)$. Let $s = [s_1, s_2, s_3, \dots s_N]$ be a vector of independent component signals, $x = [x_1, x_2, x_3, \dots x_M]$ be a vector of measured multi-channel signals, then

$$x = A * s \tag{3.2}$$

where A is the mixing matrix, which should be estimated in signal separation process. Define $y = [y_1, y_2, y_3, \dots y_N]$ the vector of estimation of the independent component signals s, then

$$y = W * x \tag{3.3}$$

where W is the separating matrix, and $W = A^{-1}$.

The fast fixed-point ICA (FastICA) algorithm assumes that when a set of non-Gaussian signals get into mixtures, it is closer to following a Gaussian distribution. Therefore, the non-Gaussianization can separate the mixtures into independent component signals. To measure the non-Gaussianity of signals, negentropy is always used in ICA. [22, 23]

$$J(y) = H(y_{Gauss}) - H(y) \tag{3.4}$$

where y_{Gauss} is a Gaussian random variable which has same covariance matrix with y. And $H(y)$ is the differential entropy with the definition

$$H(y) = -\int p_y(\eta) log p_y(\eta) d\eta \tag{3.5}$$

In FastICA algorithm, the approximation of negentropy is defined as [22, 23]

$$J(y) \propto [E\{G(y)\} - E\{G(v)\}]^2 \tag{3.6}$$

where the mean of y, v are zero and y, v are unit variance. And G can be any non-quadratic function. In FastICA, G is suggested to be

$$G_1(y) = \frac{1}{a_1} log\, cosh(a_1 y),\ G_2(y) = -exp(\frac{-y^2}{2}) \tag{3.7}$$

where $1 \leq a_1 \leq 2$, and it is usually selected to be 1.

In FastICA algorithm, the separating matrix w is obtained in an iterative process. In fixed-point update process, the update function is

$$w \leftarrow E\{zg(w^T z)\} - E\{g'(w^T z)\}w \tag{3.7}$$

where $g(y)$ can be

$$g_1(y) = tanh(a_1 y),\ g_2(y) = exp(-y^2/2),\ g_3(y) = y^3 \tag{3.8}$$

3.2. Frequency Domain Independent Component Analysis (ICA-FD)

Frequency domain independent component analysis (ICA-FD) is used to deal with convolutive signal mixing problem, which arises when there is a time delay resulting from large distance signal transmission or reflections. In ICA-FD method, the signals are separated in frequency domain. Therefore, there are several steps. Firstly, the signals are transferred into frequency domain. After that, the signals are separated in each frequency bin. Because separation is done in each frequency bin independently, the permutations in each frequency bin are different. However, the separating vectors should have same order. Thus, permutation indeterminacy and scaling ambiguity are solved in next step.

3.2.1 Separation

In convolutive signal mixing problem, if we define $h_{ij}(\tau)$ the impulse response from source j to sensor i, the measured multi-channel signals can be expressed by [23, 24]

$$x_i(t) = \sum_{j=1}^{N} \sum_{\tau} h_{ij}(\tau) s_j(t-\tau) \tag{3.9}$$

where j is the serial number of the independent source signals ($1 \le j \le 2$), i is the serial number of the measured multi-channel signals ($1 \le i \le M$). Let $s = [s_1, s_2, s_3, \dots s_N]$ is a vector of independent component signals, $x = [x_1, x_2, x_3, \dots x_M]$ is a vector of measured multi-channel signals, then

$$x(t) = \sum_{\tau} h(\tau) s(t - \tau) \tag{3.10}$$

where $h(\tau)$ is the mixing matrix. Define $y = [y_1, y_2, y_3, \dots y_N]$ the vector of estimation of the independent component signals s, $y_j(t)$ can be expressed by

$$y_j(t) = \sum_{i=1}^{M} \sum_{\tau} b_{ji}(\tau) x_i(t - \tau) \tag{3.11}$$

where $b_{ji}(\tau)$ is the impulse response in separation process.

In ICA-FD, y is estimated in frequency domain. Therefore

$$x_i(n, f) = \sum_{j=1}^{N} h_{ij}(f) s_j(n, f) \tag{3.12}$$

where $x_i(n, f)$ is the short-time Fourier transform (STFT) result of $x_i(t)$, $s_j(n, f)$ is STFT result of $s_j(t)$. $f = 1, \dots, F$ is the frequency bin index and $n = 1, \dots, N$ is the frame index. And $h_{ij}(f)$ is the impulse response in frequency domain.

In frequency domain, the measured multi-channel signals can be written by

$$X(k, f) = H(f) S(k, f) \tag{3.13}$$

Separation process can be applied in each frequency bin, and

$$Y(k, f) = W(f) X(k, f) \tag{3.14}$$

where $Y(k, f)$ is the estimation of independent component signals and $W(f)$ is the separation matrix in each frequency bin.

In frequency domain, the signals are complex valued, so complex-valued ICA is applied in ICA-FD. One of the most popular method is complex-valued FastICA algorithm (c-FastICA). In complex value signal separation, kurtosis of the signals can be used as a measure of non-Gaussianity. Kurtosis is defined by [23, 24]

$$kurt(y) = E\{|y|^4\} - 2(E\{|y|^2\}) - |E\{y^2\}|^2 = E\{|y|^4\} - 2 \quad (3.15)$$

In c-FastICA, the approximation of kurtosis is defined as [23, 24]

$$J(w) = E\{G(|w^H x|^2)\} \quad (3.16)$$

where G is a smooth even function and $\|w\| = 1$. In c-FastICA, G is suggested to be

$$G_1(y) = \sqrt{a_1 + y},\ G_2(y) = log(a_2 + y),\ G_3(y) = \frac{1}{2}y^2 \quad (3.17)$$

where a_1 and a_2 can be any constant value. They are usually selected to be 0.01. The separating matrix w is obtained in an iterative process. In fixed-point update process, the update function is

$$w \leftarrow E\{y(w^H x)^* g(|w^H x|^2)\} - E\{g(|w^H x|^2) + |w^H x|^2 g'(|w^H x|^2)\}w \quad (3.18)$$

where $y = w^H x$. And

$$g(t) = \frac{1}{(0.01+t^2)}\ ,\ g'(t) = \frac{0.5}{(0.01+t^2)^2} \quad (3.19)$$

After each iteration, there is a decorrelate process

$$W = W(W^H W)^{-1/2},\ W(f) = W(f)U(f) \quad (3.20)$$

3.2.2 Permutation

In ICA-FD, the signals are separated in each frequency bin independently. Thus after separation, the signals will be placed randomly. However, the separating vectors should have same order. Therefore, permutation indeterminacy problem occurs after that. In this part, power ratio method is applied to solve permutation indeterminacy problem.

The power ratio between the i-th separated signal and the power sum of all separated signals [27]:

$$powRatio_i(n,f) = \frac{\|a_i(f)y_i(n,f)\|^2}{\sum_{k=1}^{N}\|a_k(f)y_k(n,f)\|^2} \tag{3.21}$$

where $0 \leq powRatio_i \leq 1$. If the i-th signal is dominant, it will be closer to 1. And in frequency domain signal separation process, there is always one separated signal is dominant.

The correlation coefficient ρ between two real-valued sequences is

$$\rho(v_i, v_j) = \frac{r_{ij} - \mu_i\mu_j}{\sigma_i\sigma_j} \tag{3.22}$$

where v_i and v_j are two real-valued sequences and $r_{ij} = E\{v_i v_j\}$, $\mu_i = E\{v_i\}$, $\sigma_i = \sqrt{E\{{v_i}^2\} - {\mu_i}^2}$.

In this paper, the correlation coefficients of power ratios should be calculated. Therefore, the two real-valued sequences are defined by power ratios:

$$v_i^f(n) = powRatio_i(n,f) \tag{3.23}$$

[28] introduced two optimization techniques: global optimization and local optimization. This research applies global optimization method in permutation process. In global optimization, the cost function can be maximized:

$$\Gamma\left(\{c_k\},\{\Pi_f\}\right) = \sum_{f\in F}\sum_{k=1}^{N}\rho\left(v_i^f, c_k\right)|_{i=\Pi_f(k)} \tag{3.24}$$

where $c_k(n) \leftarrow \frac{1}{|F|}\sum_{f\in F} v_i^f(n)|_{i=\Pi_f(k)}, \forall k, n$, $\Pi_f \leftarrow \underset{\Pi}{arg\,max}\sum_{k=1}^{N}\rho(v_i^f, c_k)|_{i=\Pi_f(k)}, \forall f \in F$. And these two equations are iterated until convergence.

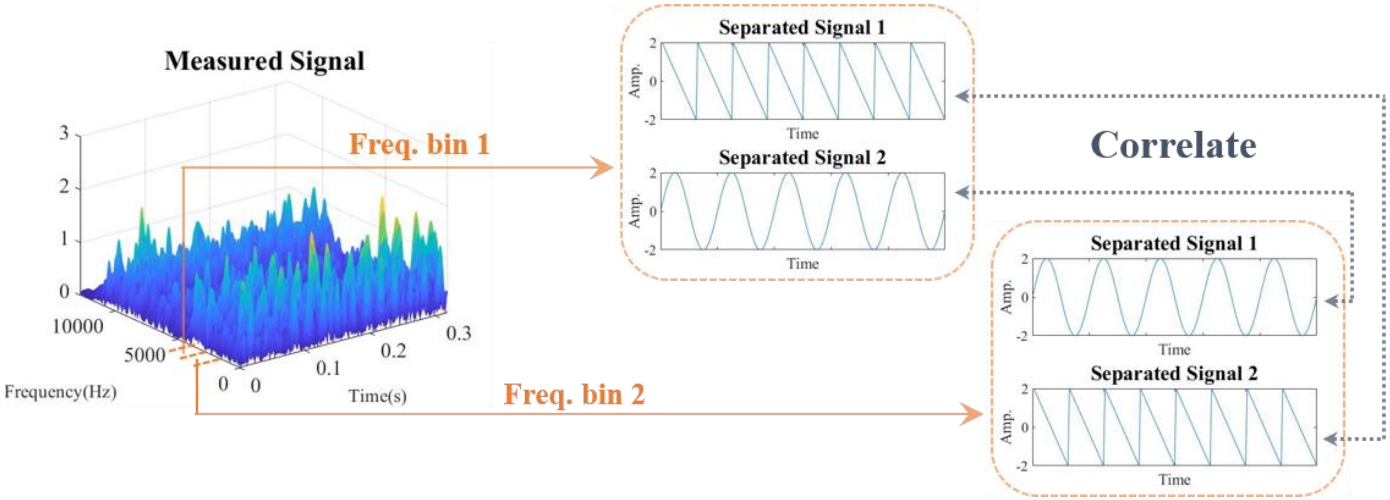

Figure 3-1 Permutation Problem in Signal Separation

3.2.3 Scaling

In ICA-FD, scaling ambiguity always occurs after separation. If $W(f)$ is the mixing matrix, when the rows of it are exchanged or multiplied by a constant, it is still a mixing matrix. In this case, permutation matrix is denoted by $P(f)$, and scaling matrix is denoted by a diagonal matrix $\Lambda(f)$.

With the permutation problem, the mixing matrix can be updated by [28]

$$W(f) \leftarrow P(f)W(f) \tag{3.25}$$

If $H(f)$ is the unknown mixing matrix, then

$$\Lambda(f)W(f)H(f) = diag[H(f)] \tag{3.26}$$

We define $W(f)H(f) = D(f)$ where $D(f)$ is a diagonal matrix. Thus

$$H(f) = W^{-1}(f)D(f) \tag{3.27}$$

With all equations, the updating process is expressed by

$$W(f) \leftarrow diag[W^{-1}(f)]W(f) \tag{3.28}$$

Therefore, scaling ambiguity problem is solved with applying inverse DFT to $W_{ij}(f)$.

3.3. Multi-stage Independent Component Analysis (MSICA)

As mentioned before, MSICA contains ICA-FD and ICA-TD [25]. The first stage is ICA-FD, which separates measured signals in frequency domain. ICA-FD is a high-stability method that can deal with convolutive mixing problem which results from large distance signal propagation or reflections.

The outputs of first stage are regarded as the input of second stage. The second stage is ICA-TD, which separates signals in time domain. ICA-TD is an efficient method which can remove the residual mixed components.

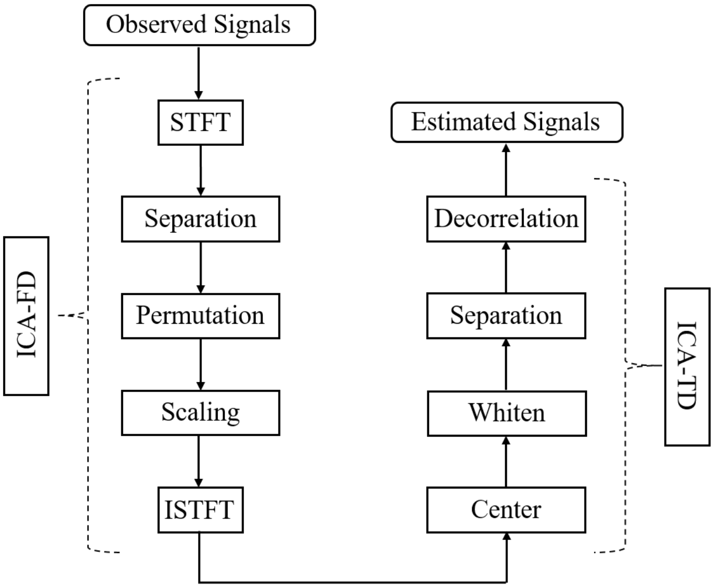

Figure 3-2 Overall procedures for vibration signal separation for the industrial robot gearboxes

Chapter 4. Experiment Evaluation

4.1 Experiment with MSICA

4.1.1 Experiment Process

To experimentally evaluate the multi-stage independent component analysis (MSICA), vibration signals measured on Hyundai industrial robot are analyzed. The industrial robot and its two gearboxes are shown in Figure 2-1. The closest axis to robot basement is named as 1st axis which is the heaviest axis. The 4th and 5th axis are close to the robot gripper, which are lighter axes. Two vibration sensors are attached on 4th gearbox and 5th gearbox for detecting vibration signals from gearbox shell. The vibration signals contain the signals from bearings, gears and so on. Therefore, the vibration signals measured from sensors can be used to diagnosis the faults of gearbox components.

Due to small weights, the vibration amplitudes of 4th and 5th gearbox are large. And because of short distance between two axes, the vibration can influent each other. From Figure 2-1(b), it can be found that the distance between two gearboxes is resembling to the size of gearboxes. So the distances between components of gearboxes are different. Therefore, there can be convolutive vibration signal mixtures.

In the experiment, two vibration sensors are attached on 4th and 5th gearbox to obtain vibration signals. The sampling rate of sensors is 25,600 Hz. Four comparison experiments are conducted in this subsection. The first experiment is conducted with normal bearings and gears. But in the second experiment, the faulty bearing is in 4th gearbox. And in the third and four experiments, only 4th axis and 5th axis have motions. The third and four experiment modes are defined as single motion. And vibration signals are extracted from corresponding gearboxes, which are defined as single motion signals. The single motion signals are regarded as reference signals in this experiment, because there is no multi-axis interference participating in the single motion mode experiment.

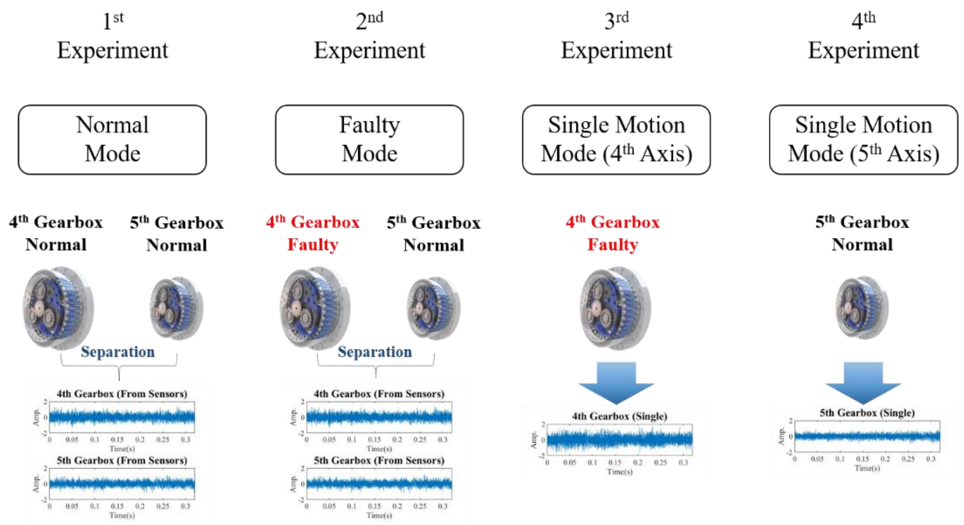

Figure 4-1 Four experiment modes

Figure 4-2 demonstrates the rotation speed profiles of two axes. The maximum rotation speed is 2 revolutions per second (RPS). The vibration signals acquired from two sensors in the faulty mode are shown in Figure 4-3. The measured signals have constant speed components and varying speed components. However, variable speed will influence the diagnosis results. Therefore, only constant speed vibration signals are analyzed in experiment. Separation process and features extraction should be conducted in constant speed components of measured vibration signals.

Figure 4-4 shows the constant speed signals and their frequency domain spectrums. The first row represents 4th gearbox and the second row is 5th gearbox. As shown in 4-4(b), both signals have high amplitude at 300Hz. And 4th gearbox signal also shows high amplitude at 2,500Hz and 4,000Hz. 5th gearbox signal has high amplitude at 1,800Hz, 3,000Hz, 3,800Hz, 4,800Hz and 5,000Hz.

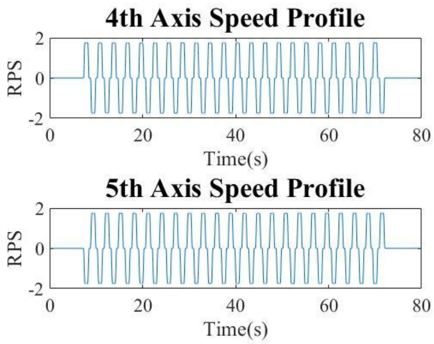

Figure 4-2 Speed profile of 4th axis and 5th axis

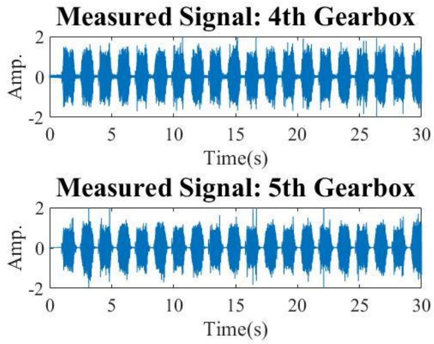

Figure 4-3 Vibration signals measured from 4th axis and 5th axis

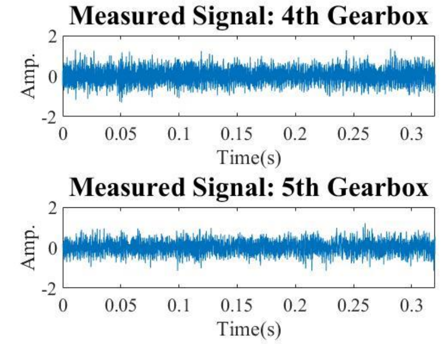

(a)

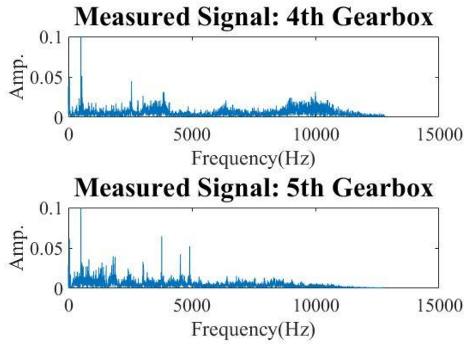

(b)

Figure 4-4 (a) Constant speed vibration signals, and (b) their spectrums

In the 1st stage, the signals are transferred into time-frequency domain by using short-time Fourier transform (STFT). The time-frequency spectrums of original measured signals are shown in Figure 4-5. X axis is time, and Y axis is frequency. The amplitude can be recognized by colors. The certain components of two signals are same in same time-frequency bins due to the signal mixing problem, especially at 300Hz, which show high amplitude in same time-frequency bins.

In the first stage, ICA-FD is applied in each frequency bin. ICA-FD divides signals into 8,192 frequency bins. Signal separation, permutation and scaling process are conducted in each frequency bin. Figure 4-6 shows the time-frequency spectrums of separated signals after 1st stage. Traces of separation are clearly shown in the plots. The accuracy of this separation process cannot be demonstrated clearly in the spectrums, because the signals are extremely complex. But the accuracy of the method will be analyzed in next step.

After separation in time-frequency domain, the separated signals are transferred back to time domain by using inverse short time Fourier transform (ISTFT). The estimated time domain signals after 1st stage are shown in Figure 4-6(a).

In the 2nd stage, ICA-TD is applied in time domain. Because the output of the 1st stage is the input of 2nd stage. Therefore, Figure 4-7(a) is also regard as the input of ICA-TD. And the estimated signals after 2nd stage are shown in Figure 4-7(b). Thus, Figure 4-7(b) is the final estimated signals after MSICA method. Features should be extracted in this final estimated signals. Figure 4-8 shows the whole separation process of MSICA in this experiment.

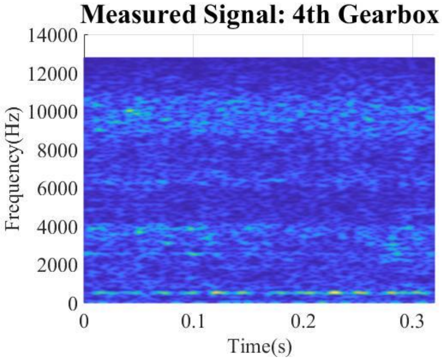

(a)

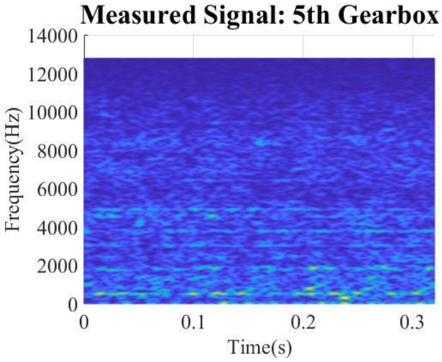

(b)

Figure 4-5 Measured vibration signals in time-frequency domain: (a) 4th gearbox, (b) 5th gearbox

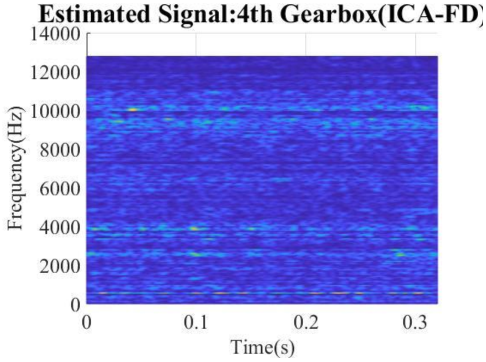

(a)

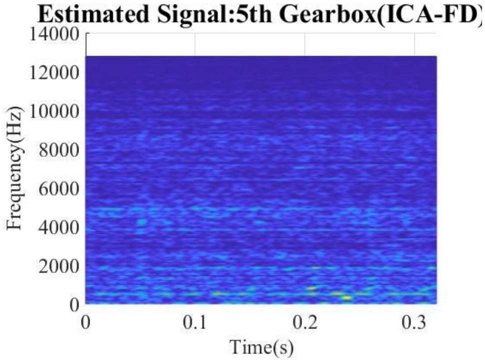

(b)

Figure 4-6 Estimated independent source signals in time-frequency domain: (a) 4th gearbox, (b) 5th gearbox

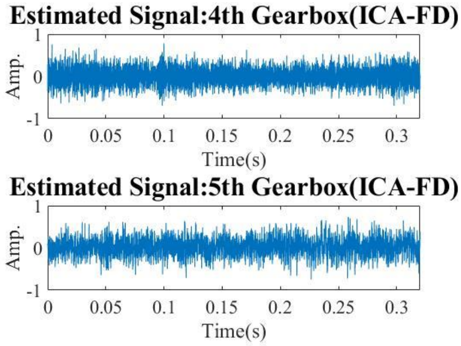

(a)

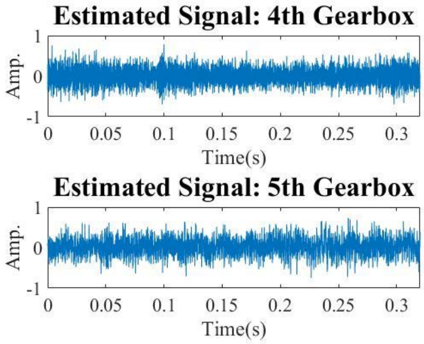

(b)

Figure 4-7 (a) Estimated independent source signals after ICA-FD, (b) Estimated independent source signals after MSICA

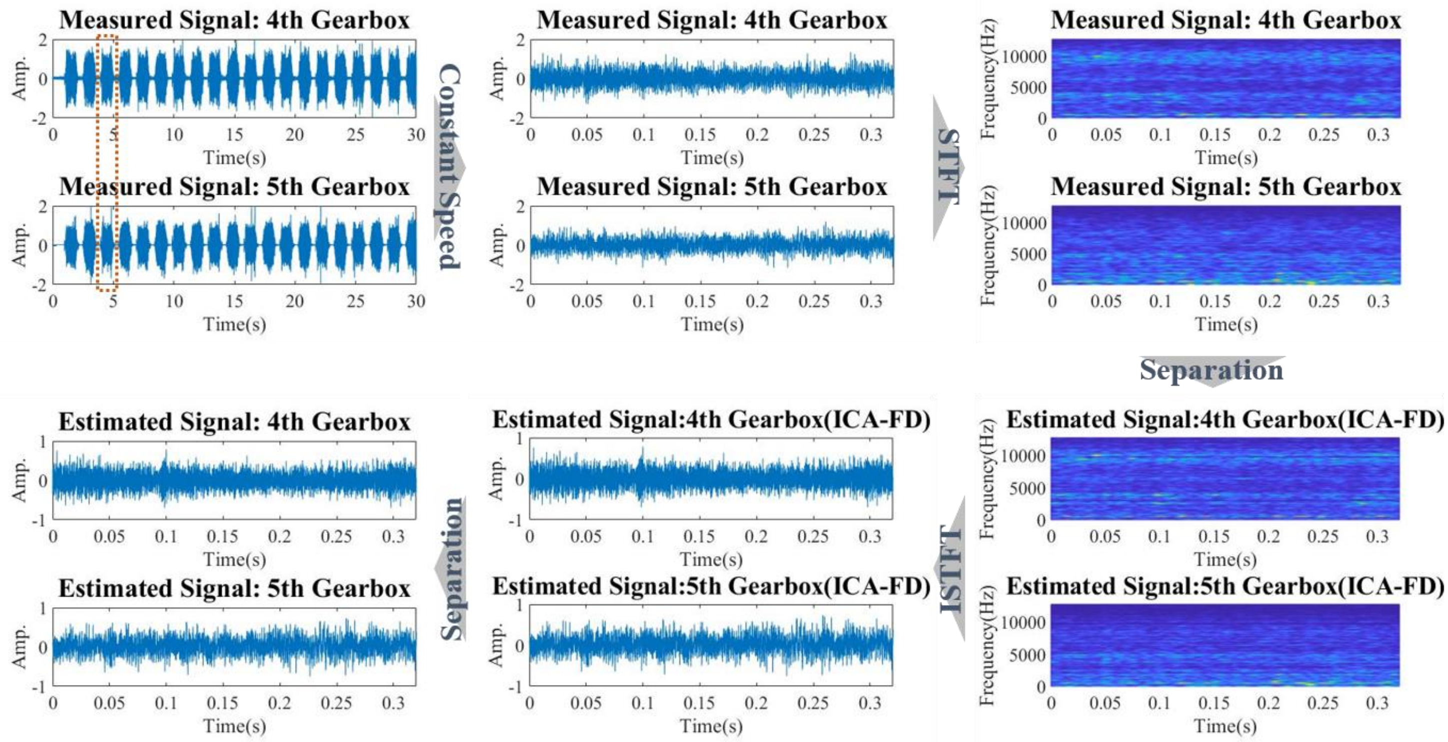

Figure 4-8 Flow Chart of Separation Process in Experiment

4.1.2 Result Analysis

To confirm the validity and accuracy of MSICA method, the frequency spectrums of vibration signals are drawn. The frequency spectrums of final estimated vibration signals are shown in Figure 4-9. And because there is no multi-axis interference in the single motion experiments. Therefore, single motion signals can be regarded as correct vibration signals. The frequency spectrum of single motion signals can be used to compared with final estimated signals to confirm the validity of MSICA in industrial robot fault detection. Figure 4-10 shows the frequency spectrums of single motion signals. The comparison of estimated signals and single motion signals is shown in Figure 4-11.

As shown in Figure 4-9 and Figure 4-11, the estimated signals have same trend with single motion signals for both axes. Especially, the high amplitude components are located in same frequencies. For instance, the high amplitude in 300Hz is eliminated in 4th gearbox vibration signal but still remains in 5th gearbox signal, which is same with single motion vibration signals. Therefore, MSICA can restore the vibration signals and can separate the signals correctly in 300Hz frequency bin.

To confirm the performance of MSICA in industrial robot fault diagnosis, RMS features are extracted in the 1st experiment and the 2nd experiment which are performed in normal mode and faulty mode. The comparison of root mean square (RMS) and the comparison of RMS ratio of two experiments are shown in Figure 4-12 and Figure 4-13. In RMS feature calculation, more than 8 constant speed intervals of vibration signals are analyzed, where the results are convincing.

RMS reflects energy of vibration signals in time domain [29]. Therefore, when RMS feature increase a lot, the mechanism component can be defined as a faulty component. Thus, RMS ratio can show the results more clearly, which is the ratio between RMS in faulty mode and RMS in normal mode. When RMS ratio is close to 1, the component can be defined in normal condition.

As demonstrated in Figure 4-12 and Figure 4-13, the diagnosis results show that both gearboxes are faulty from measured signals without MSICA method. However, with MSICA technique separating the measured signals, RMS ratio of 5th gearbox becomes close to 1 which is same with real situation. And 4th gearbox is still a faulty gearbox with MSICA method. Therefore, from this result, it can be found that MSICA method is effective in separating the vibration signals for gearbox diagnosis in industrial robots.

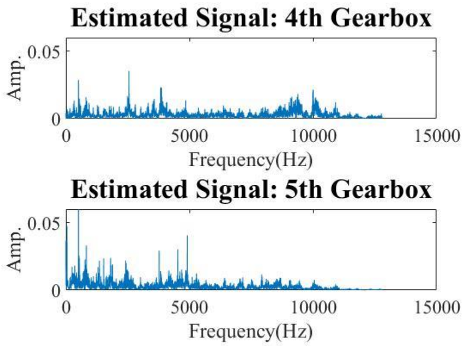

Figure 4-9 The spectrum of final estimated independent source signals

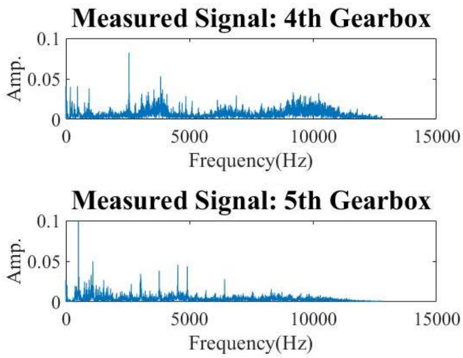

Figure 4-10 The spectrum of single motion signals

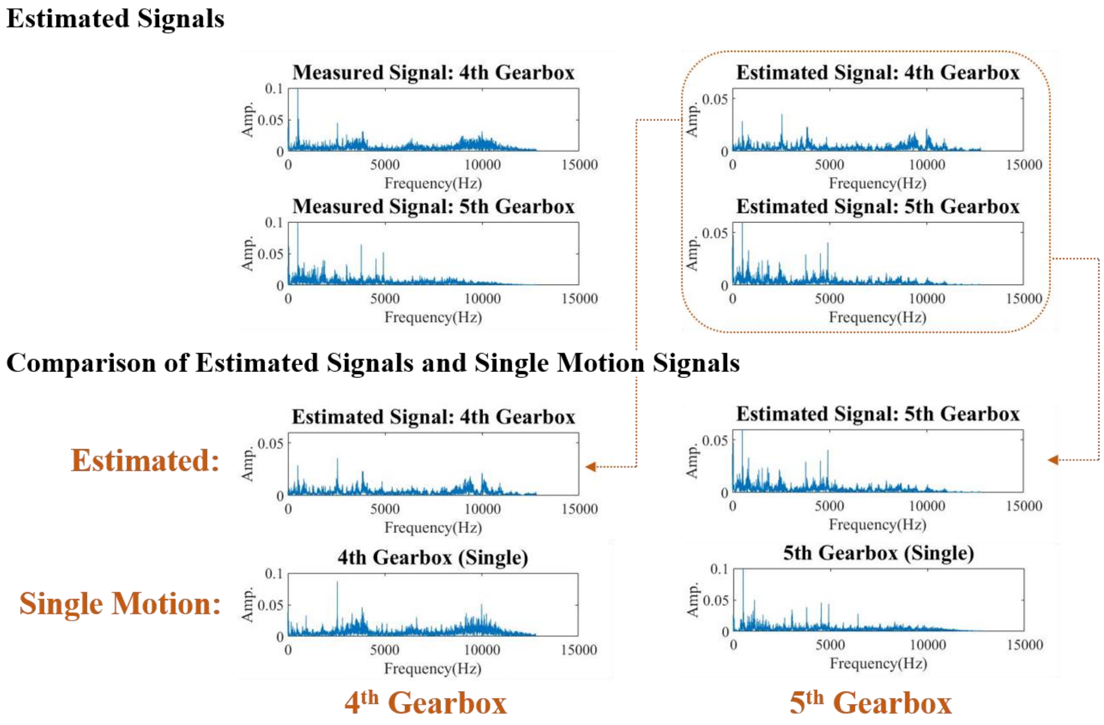

Figure 4-11 Comparison of Estimated Signals and Single Motion Signals

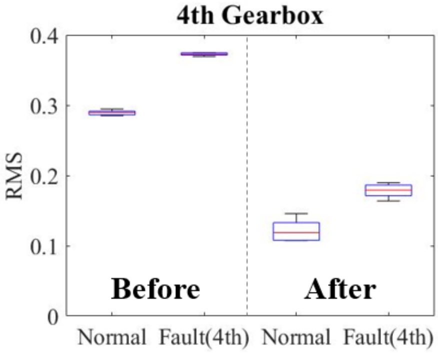

(a)

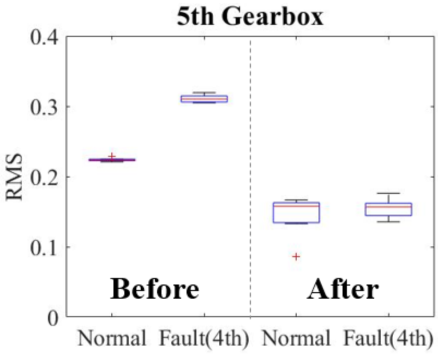

(b)

Figure 4-12 Comparison of RMS: (a) 4th gearbox, (b) 5th gearbox

Before - before the method; After - After the method; Fault(4th) - when 4th gearbox is faulty

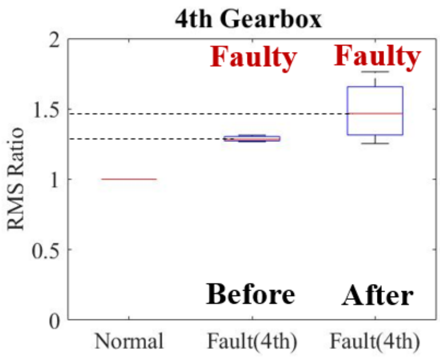

(a)

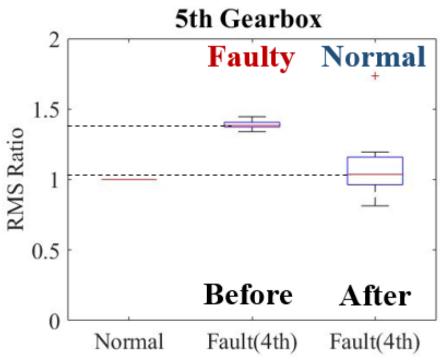

(b)

Figure 4-13 Comparison of RMS ratio: (a) 4th gearbox, (b) 5th gearbox

Before - before the method; After - After the method; Fault(4th) - when 4th gearbox is faulty

4.2 Comparison Experiment Using Basic ICA Method

The comparison experiment is conducted in this research. The experiment is designed to compare the efficiency of MSICA method and basic ICA method in fault detection of gearboxes in industrial robots. The basic ICA is the method which separates the signals in time domain using FastICA algorithm. In this experiment, the same vibration signals are selected to do analysis. Thus, the faulty bearing is still in 4th gearbox, and 5th gearbox is in normal condition. And experiments in four experiment modes are conducted in this subsection. The separation process of basic ICA method is drawn in Figure 4-14.

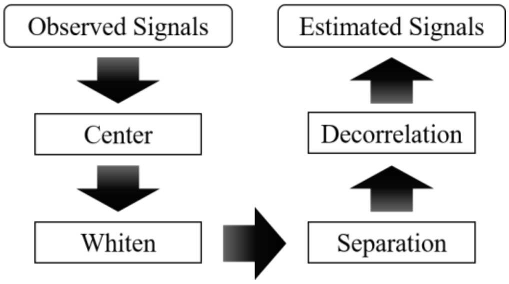

Figure 4-14 Separation process of basic ICA method

The observed vibration signals are shown in Figure 4-15(a) and estimated vibration signals using ICA method are shown in Figure 4-15(b). The spectrums of measured and estimated vibration signals using ICA are shown in Figure 4-16.

As shown in Figure 4-16(b), the estimated vibration signal of 4th gearbox has high amplitude at 4,500Hz and 4,800Hz, which is not correct separation result. Because the measured 4th gearbox signal does not have high amplitude at 4,500Hz and 4,800Hz. And also the estimated vibration signal of 4th gearbox has high amplitude at 300Hz, which is different with the single motion signals. And the estimated vibration signal of 5th gearbox has wrong amplitude at 300Hz. Therefore, basic ICA method cannot separate the vibration signals correctly.

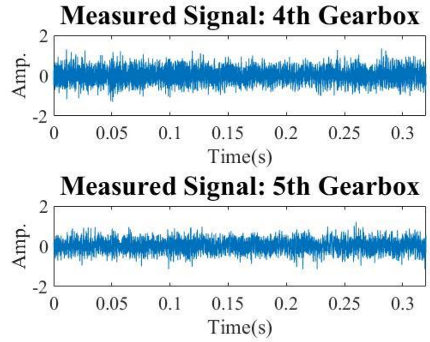

(a)

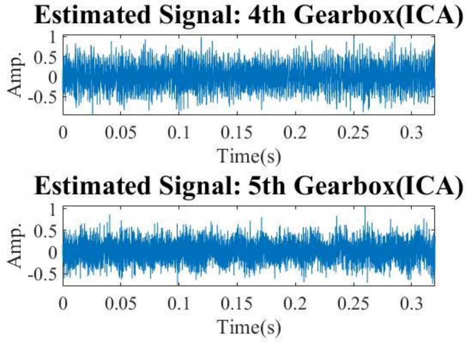

(b)

Figure 4-15 (a) Observed vibration signals, (b) Estimated vibration signals using ICA method

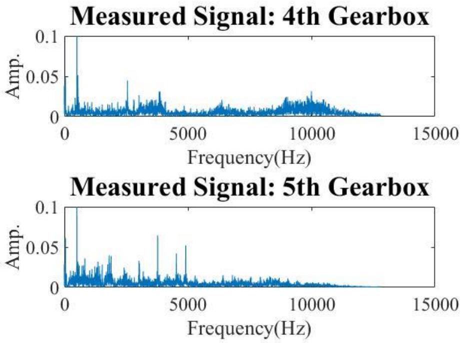

(a)

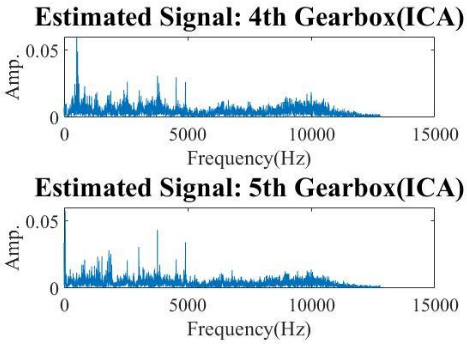

(b)

Figure 4-16 (a) Spectrums of observed signals, (b) Spectrums of estimated signals using ICA method

To further confirm the results, the comparison of RMS of 4th gearbox and 5th gearbox using ICA method are shown in Figure 4-17 and Figure 4-18. As demonstrated in Figure 4-17 and Figure 4-18, the diagnosis results show that both gearboxes are faulty from measured signals without any separation method. However, with basic ICA, both of them are still faulty, which is different from the real situation. The figure also shows that basic ICA method cannot correctly separate the vibration signals for gearbox diagnosis in industrial robots.

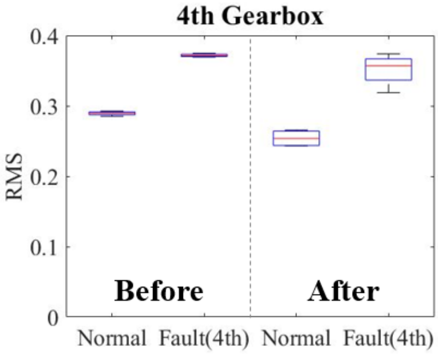

(a)

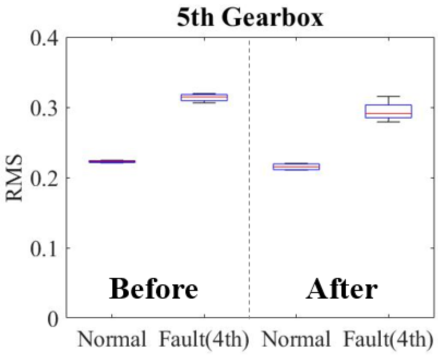

(b)

Figure 4-17 Comparison of RMS using ICA method: (a) 4th gearbox, (b) 5th gearbox

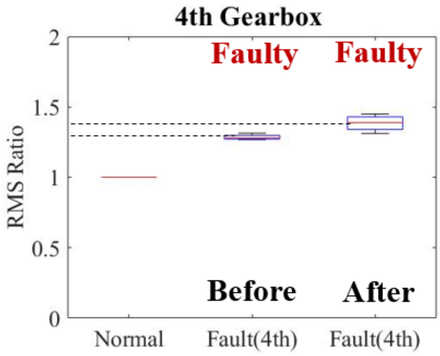

(a)

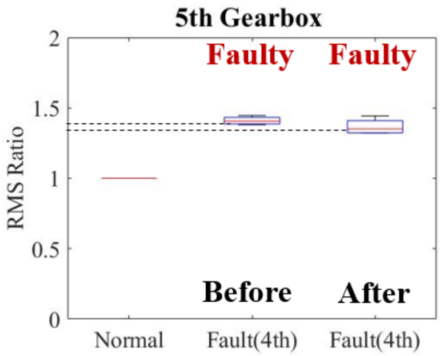

(b)

Figure 4-18 Comparison of RMS ratio using ICA method: (a) 4th gearbox, (b) 5th gearbox

4.3 Comparison Experiment Using ICA-FD Method

The experiment is designed to compare the efficiency of ICA-FD and MSICA in fault detection of gearboxes in industrial robots. The ICA-FD is the method which separates signals in frequency domain. In this experiment, the same vibration signals are selected to be analyzed. Therefore, the faulty bearing is still in 4th gearbox, and 5th gearbox is still in normal condition. And experiments in four experiment modes are conducted in this subsection. The separation process of ICA-FD method in shown in Figure 4-19.

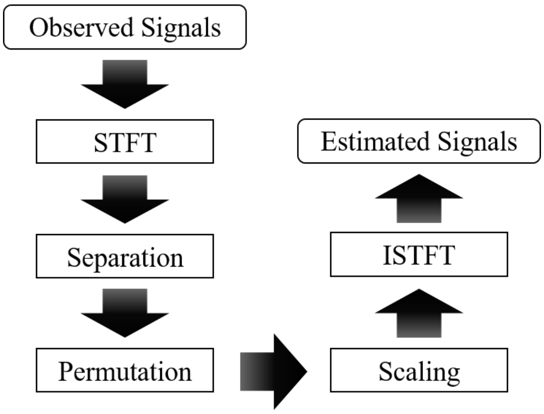

Figure 4-19 Separation process of ICA-FD method

The measured vibration signals are shown in Figure 4-20(a) and estimated vibration signals using ICA-FD method are shown in Figure 4-20(b). The spectrums of measured signals and estimated signals using ICA-FD method are shown in Figure 4-21. In Figure 4-21(b), the estimated signals using ICA-FD have same spectrums with single motion signals, which are shown in Figure 4-10. Therefore, the effect of ICA-FD method cannot be easily distinguished in the spectrums due to the complex vibration signals. In this case, RMS feature calculation results can be used to examine the effect differences between ICA-FD and MSICA.

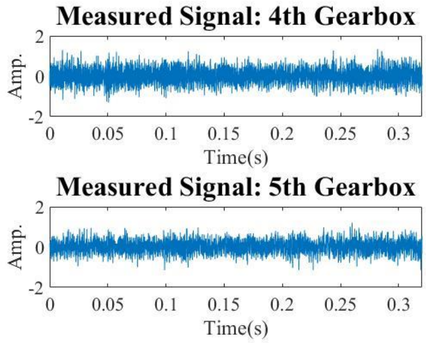

(a)

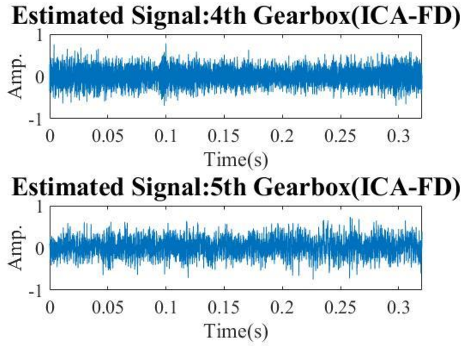

(b)

Figure 4-20 (a) Observed vibration signals, (b) Estimated vibration signals using ICA-FD method

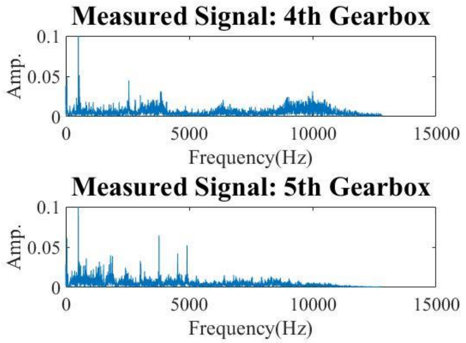

(a)

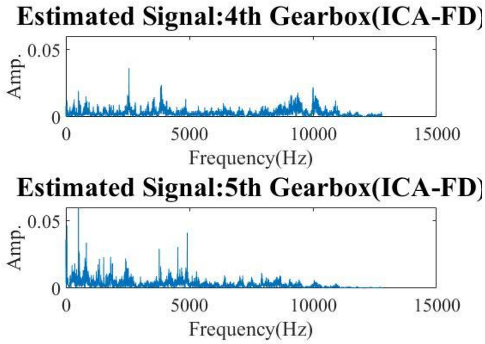

(b)

Figure 4-21 (a) Spectrums of observed signals, (b) Spectrums of estimated signals using ICA-FD method

The comparisons of RMS and RMS ratio between 4th axis gearbox and 5th axis gearbox after ICA-FD method are shown in Figure 4-22 and Figure 4-23. As shown in the figures, ICA-FD could separate the vibration signals correctly in this experiment. RMS feature calculation results show that both gearboxes are faulty from original measured signals. However, with ICA-FD method, the result shows 4th gearbox is faulty and 5th gearbox is in normal situation, which is same with the real situation.

Figure 4-24 shows the comparison of RMS ratio in 5th axis gearbox using ICA-FD and MSICA method. As demonstrated in Figure 4-24, ICA-FD could eliminate partial multi-axis interference. However, compared with MSICA, ICA-FD is less efficient in vibration signal separation in industrial robots. And MSICA can eliminate more interference from 4th gearbox since RMS feature of MSICA shows better results. Because the 2nd stage of MSICA method can eliminate the residual mixed components. Therefore, compared with ICA-FD, the efficiency of MSICA is better when applied into industrial robots.

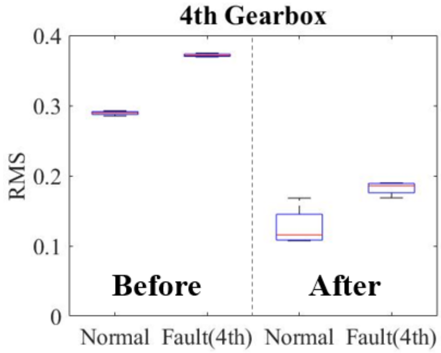

(a)

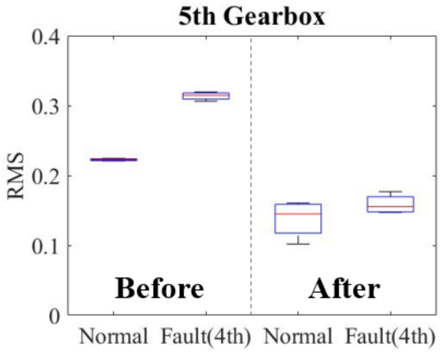

(b)

Figure 4-22 Comparison of RMS using ICA-FD method: (a) 4th gearbox, (b) 5th gearbox

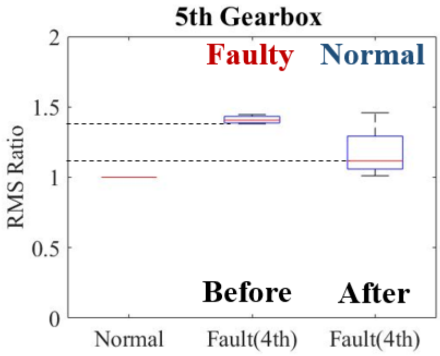

(a)

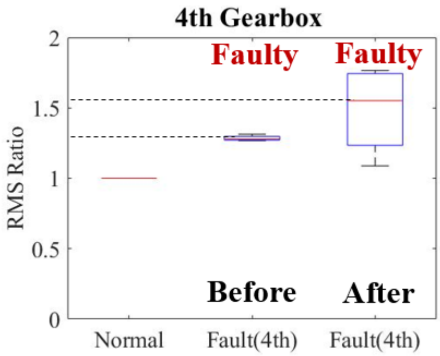

(b)

Figure 4-23 Comparison of RMS ratio using ICA-FD method: (a) 4th gearbox, (b) 5th gearbox

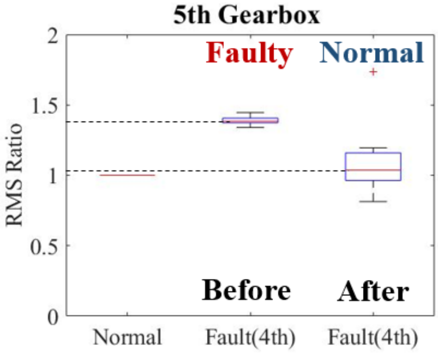

(a)

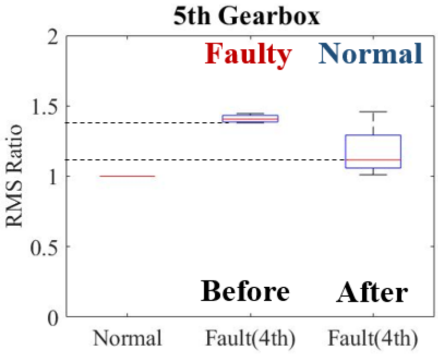

(b)

Figure 4-24 Comparison of RMS ratio in 5th axis gearbox using (a) FDICA and (b) MSICA method

Chapter 5. Discussion and Conclusion

5.1 Conclusions and Contributions

A vibration signal separation method for gearbox fault diagnosis in industrial robots was presented in this research by using multi-stage independent component analysis technique which has two stages. The first stage is frequency domain independent component analysis, which is aiming to separate the convolutive mixture. The second stage is time domain independent component analysis, which is aiming to separate linear mixture and remove the residual mixed components.

The experiment results showed the efficiency of this method in robot fault diagnosis. In the experiment, the faulty gear is in 4th gearbox. However, without MSICA method, the vibration signals from 4th gearbox and 5th gearbox are mixed with each other. The fault detection results show that both gearboxes are faulty. But in the experiment, MSICA separates the mixed vibration signals. And it shows that only 4th gearbox is faulty but 5th gearbox is normal case, which is correct result and same with the real situation. And also, as shown from the frequency spectrums of measured signals and estimated signals, MSICA method separates vibration signals correctly. Thus, MSICA is a suitable technique in industrial robot fault detection.

Therefore, from the experiment results, the following conclusions can be drawn:

(1) MSICA method can separate the vibration signals successfully in industrial robot from mixed signals, which are measured from vibration sensors attached on 4th axis and 5th axis.

(2) The technique can correctly get the diagnosis result, which is same with the real condition.

(3) Compared with basic ICA method and ICA-FD method, MSICA method is more suitable when applied into industrial robots.

5.2 Future Work

1) Combine machine learning with time-frequency domain mask, to improve the efficiency of vibration signal separation. [30]

    In speech separation, there is a more efficient method to separate speech signals. time-frequency domain mask is a mask multiplied to time-frequency spectrum of original measured signals. The separation process is extremely efficient due to the simple calculation process. However, the limitation of time-frequency domain mask is that there must be a train set for machine learning which includes single motion signals and measured mixed signals. But this issue will bring more difficulties for experiments. Because the time series of single motion signals should be simultaneous with measured mixed signals. With this problem solved, time-frequency domain mask will be an efficient method to eliminate multi-axis interference in industrial robot fault detection.

2) Application of this technique into general motions.

    The experiment is conducted with 4^{th} gearbox and 5^{th} gearbox, and it is confirmed that the multi-axis interference and separation process cannot influence other gearboxes. Therefore, this method can be applied into general motions and real manufacturing process where all axes have motions.

Bibliography

[1] M. A. K. Bahrin, M. F. Othman, N. N. Azli, and M. F. Talib, "Industry 4.0: A review on industrial automation and robotic," *Jurnal Teknologi,* vol. 78, no. 6-13, pp. 137-143, 2016.

[2] J. Huang, Y. Wang, and T. Fukuda, "Set-membership-based fault detection and isolation for robotic assembly of electrical connectors," *IEEE Transactions on Automation Science and Engineering,* vol. 15, no. 1, pp. 160-171, 2016.

[3] S. Bajaj, "Industrial Robotics Market by Type (Articulated robots, Cylindrical robots, Selective Compliant Assembly Robot Arm (SCARA) robots, Cartesian robots, and other types), End user (automotive, electrical & electronics, chemical, rubber & plastics, machinery, metals, food & beverages; precision & optics, and others), Function(soldering & welding, materials handling, assembling & disassembling, painting & dispensing, milling, cutting & processing, and others) and Geography - Global Opportunity Analysis and Industry Forecast, 2017-2023," 2017.09. [Online]. Available: https://www.alliedmarketresearch.com/industrial-robotics-market

[4] W. Sundblad, "What's At Stake In The Race To Industry 4.0?," 2018.07.30. [Online]. Available: https://www.forbes.com/sites/willemsundbladeurope/2018/07/30/whats-at-stake-in-the-race-to-industry-4-0/#ef85ad37d11e

[5] L. Cruz, "Digitization and IoT reduce production downtime," 2016.03.16. [Online]. Available: https://newsroom.cisco.com/feature-

content?type=webcontent&articleId=1764957

[6] B. Xiao and S. Yin, "An intelligent actuator fault reconstruction scheme for robotic manipulators," *IEEE transactions on cybernetics,* vol. 48, no. 2, pp. 639-647, 2017.

[7] D. Brambilla, L. M. Capisani, A. Ferrara, and P. Pisu, "Fault detection for robot manipulators via second-order sliding modes," *IEEE Transactions on Industrial Electronics,* vol. 55, no. 11, pp. 3954-3963, 2008.

[8] A. A. Jaber and R. Bicker, "Fault diagnosis of industrial robot gears based on discrete wavelet transform and artificial neural network," *Insight-Non-Destructive Testing and Condition Monitoring,* vol. 58, no. 4, pp. 179-186, 2016.

[9] J. Lee, F. Wu, W. Zhao, M. Ghaffari, L. Liao, and D. Siegel, "Prognostics and health management design for rotary machinery systems—Reviews, methodology and applications," *Mechanical systems and signal processing,* vol. 42, no. 1-2, pp. 314-334, 2014.

[10] J. M. Ha, J. Park, K. Na, Y. Kim, and B. D. Youn, "Toothwise fault identification for a planetary gearbox based on a health data map," *IEEE Transactions on Industrial Electronics,* vol. 65, no. 7, pp. 5903-5912, 2017.

[11] J. M. Ha, B. D. Youn, H. Oh, B. Han, Y. Jung, and J. Park, "Autocorrelation-based time synchronous averaging for condition monitoring of planetary gearboxes in wind turbines," *Mechanical Systems and Signal Processing,* vol. 70, pp. 161-175, 2016.

[12] J. Park, J. M. Ha, H. Oh, B. D. Youn, J.-H. Choi, and N. H. Kim, "Model-

based fault diagnosis of a planetary gear: A novel approach using transmission error," *IEEE Transactions on Reliability,* vol. 65, no. 4, pp. 1830-1841, 2016.

[13] E. Olsson, P. Funk, and M. Bengtsson, "Fault diagnosis of industrial robots using acoustic signals and case-based reasoning," in *European Conference on Case-Based Reasoning*, 2004: Springer, pp. 686-701.

[14] I. Eski, S. Erkaya, S. Savas, and S. Yildirim, "Fault detection on robot manipulators using artificial neural networks," *Robotics and Computer-Integrated Manufacturing,* vol. 27, no. 1, pp. 115-123, 2011.

[15] G. Gelle, M. Colas, and G. Delaunay, "Blind sources separation applied to rotating machines monitoring by acoustical and vibrations analysis," *Mechanical Systems and Signal Processing,* vol. 14, no. 3, pp. 427-442, 2000.

[16] X. Tian, J. Lin, K. R. Fyfe, and M. J. Zuo, "Gearbox fault diagnosis using independent component analysis in the frequency domain and wavelet filtering," in *2003 IEEE International Conference on Acoustics, Speech, and Signal Processing, 2003. Proceedings.(ICASSP'03).* 2003, vol. 2: IEEE, pp. II-245.

[17] J. Leng, S. Jing, and C. Luo, "Fault Feature Extraction of Single-Channel Signal from Gearbox Based on EEMD and CICA," *Recent Advances in Electrical & Electronic Engineering (Formerly Recent Patents on Electrical & Electronic Engineering),* vol. 11, no. 1, pp. 69-75, 2018.

[18] X. Zou, P. Jancovic, J. Liu, and M. Kokuer, "Speech signal enhancement based on MAP algorithm in the ICA space," *IEEE Transactions on Signal*

Processing, vol. 56, no. 5, pp. 1812-1820, 2008.

[19] A. Subasi and M. I. Gursoy, "EEG signal classification using PCA, ICA, LDA and support vector machines," *Expert systems with applications,* vol. 37, no. 12, pp. 8659-8666, 2010.

[20] Y. Xu, S.-Q. Shen, Y.-L. He, and Q.-X. Zhu, "A Novel Hybrid Method Integrating ICA-PCA With Relevant Vector Machine for Multivariate Process Monitoring," *IEEE Transactions on Control Systems Technology,* no. 99, pp. 1-8, 2018.

[21] L. J. Stifelman, "The cocktail party effect in auditory interfaces: a study of simultaneous presentation," *Retrieved August,* vol. 2, p. 2011, 1994.

[22] A. Hyvärinen and E. Oja, "A fast fixed-point algorithm for independent component analysis," *Neural computation,* vol. 9, no. 7, pp. 1483-1492, 1997.

[23] A. Hyvärinen, J. Karhunen, and E. Oja, *Independent component analysis*. John Wiley & Sons, 2004.

[24] E. Bingham and A. Hyvärinen, "A fast fixed-point algorithm for independent component analysis of complex valued signals," *International journal of neural systems,* vol. 10, no. 01, pp. 1-8, 2000.

[25] T. Nishikawa, H. Saruwatari, and K. Shikano, "Blind source separation of acoustic signals based on multistage ICA combining frequency-domain ICA and time-domain ICA," *IEICE Transactions on Fundamentals of Electronics, Communications and Computer Sciences,* vol. 86, no. 4, pp. 846-858, 2003.

[26] M. Geravanchizadeh and M. Hesam, "Convolutive ICA for audio signals,"

in *Independent Component Analysis for Audio and Biosignal Applications*: IntechOpen, 2012.

[27] H. Sawada, S. Araki, and S. Makino, "Measuring dependence of bin-wise separated signals for permutation alignment in frequency-domain BSS," in *2007 IEEE International Symposium on Circuits and Systems*, 2007: IEEE, pp. 3247-3250.

[28] H. Sawada, R. Mukai, S. Araki, and S. Makino, "A robust and precise method for solving the permutation problem of frequency-domain blind source separation," *IEEE transactions on speech and audio processing,* vol. 12, no. 5, pp. 530-538, 2004.

[29] V. Sharma and A. Parey, "A review of gear fault diagnosis using various condition indicators," *Procedia Engineering,* vol. 144, pp. 253-263, 2016.

[30] D. Wang, "On ideal binary mask as the computational goal of auditory scene analysis," in *Speech separation by humans and machines*: Springer, 2005, pp. 181-197.